Coalescence and agglomeration of individual milk particles during convective drying
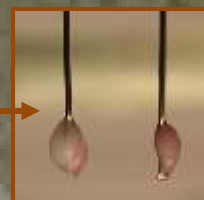
Coalescence

Stickiness

Non-stickiness

Vincenzina Robertiello

UNIVERSITÀ DEGLI STUDI DI SALERNO

Facoltà di Ingegneria
Dipartimento di Ingegneria Industriale

Master Degree in Food Engineering

Coalescence and agglomeration of individual milk particles during convective drying
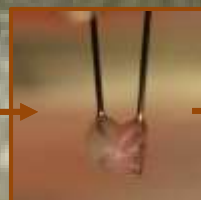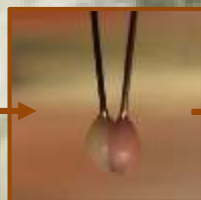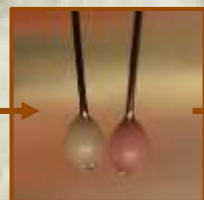
Master thesis in
Transport Phenomena in Food Processes

Relatori: Candidata:

Prof. Ing. Gaetano Lamberti   Vincenzina Robertiello

Prof. Ing. Anna Angela Barba   matricola 0622800192

Prof. Ing. Lilia Ahrné

Correlatore:

Ing. Loredana Malafronte

Anno Accademico 2015/2016

Ai miei nonni,
Vincenza e Angelo

Questo testo è stato stampato in proprio, in Times New Roman

La data prevista per la discussione della tesi è il 09/06/2016
Fisciano, 26/05/2016

Contents

List of figures

List of tables

Abstract

The goal of this research is to develop a novel methodology that combines experiments and modelling to help understand the physical conditions of the coalescence and stickiness of milk particles brought into contact in order to control the functional properties of dairy powder and design equipment.

In this work a new method to study inter-particle behavior during coalescence and stickiness of two individual particles is presented. A two individual particles drying kinetics device is successfully implemented and particles contact tests were performed. A tip with two filaments is used for the drying experiments with contact test. For each experiment, two individual particles of initial weight of about 2 mg are dried individually until a certain water content is reached. After that the chamber was closed to the air flow for 30 seconds and the particles were put into contact by bringing close the tips using tweezers, drying was then continued until the particles was dried. Experiments were performed at the air temperature of 50, 70 and 90 °C, and air velocity of 1m/s.

In order to select the direction of the air flow during drying of two particles, drying kinetics of a single particle (case I) was compared with drying kinetics of two particles in orthogonal (case II) and parallel position (case III) respect to the air flow. Comparing drying kinetics of case II and III with case I it was possible to see that case III is slower than case I instead case II showed the same drying kinetics of case I. Also the morphology of particles is different: in the case I and case II the air flow meet at the same time the droplets and they show the same morphology change; instead in the case III the particle that meets the air flow first is dryer than the second one. For this reason, the drying kinetics of case III is slower than the case I and II. These preventive tests are allowed to choose which position of particles would give us the same morphology and the same drying kinetics of a single particle. It was decided to perform the experiments placing the particles orthogonally to the air flow direction (case II).

Experiments were performed for skim and whole milk. Comparing the drying kinetics of skim milk and whole milk, which have the similar initial water content, the results showed that whole milk have a longer drying time than skim milk. The only difference between skim milk and whole milk is the fat presence that slow the drying time of the particle.

Particles contact tests, both for skim and whole milk, showed that it was possible to distinguish between three major mechanisms: coalescence, stickiness and non-stickiness. Coalescence occurs when during the contact a particle is transferred to another particle and they can merge forming a larger spherical particle. Stickiness occurs when after contact the particles change their shapes, necking appears at the interphase particle-particle while separating, which can cause deformation or breakage of particles. Non stickiness occurs when the particles after contact can separate without necking formation, and their shapes do not change. Four different cases of stickiness were observed, for a total of six particles contact cases, including coalescence and non-stickiness. Differences between cases could be related to adhesion and cohesion forces. Adhesion forces fully dominated during coalescence and gradually reduced until non-stickiness was observed, at this point cohesive forces dominated the mechanism, hence surface of particles are considered being non-sticky. Measurements of drying kinetics of particles after contact tests have showed that the device was able to capture differences in drying time. Drying kinetics particles were evaluated only for skim milk particles. Whole milk particles after contact test showed a shape and size differently than before the contact for this reason the drying rate was not considered. Skim milk particles when showed a coalescence mechanism exhibited a lower drying rate after contact test, if compared with sticky and non-sticky particles. In fact, coalescence leaded to the formation of a bigger spherical particle, which has a longer drying time. Stickiness and non-stickiness, instead, leaded to the formation of two particles with a shape and size similar to the initial particles, therefor drying rates are comparable with drying rate of a single particle.

The evaluation of the conditions of coalescence and agglomeration was carried out by associating the experimental tests to dimensionless number (Oh^2), evaluated taking into account the surface condition and the glass transition temperature (T_g). A validated drying kinetics model was used to simulate surface conditions of particles during milk drying. Contact tests were showed that particles, which exhibited coalescence had a calculated $Oh^2_{surface}$ lower than 1. This validated the theoretical criteria, which is used for modelling collision of particles during spray drying using CFD; Oh^2 has to be calculated as a function of the surface

conditions of the particles and not as a function of average conditions. In contrast, particles that showed stickiness and non-stickiness behavior had a calculated $Oh_{surface}^2$ greater than 1. Calculation of $\Delta T_{surface} = (T - T_g)_{surface}$ showed that particle coalesced for $\Delta T_{surface} > 140°C$ and they were sticky for $\Delta T_{surface} > 30°C$, which is in agreement with literature results of stickiness of amorphous materials, for which sticky point is between 20 and 40°C.

The experimental results combined with the validated drying kinetics model can be used for modelling the spray drying process. The suggested approach can be used to support the design and scale-up of the spray dryer and to enhance and control final product properties.

Riassunto

L'obiettivo di questo lavoro di tesi è stato quello di sviluppare una metodologia innovativa che combini gli esperimenti con la modellazione per aiutare a comprendere le condizioni fisiche di coalescenza e agglomerazione di particelle di latte messe in contatto al fine di controllare le proprietà funzionali del latte in polvere e il design delle apparecchiature.

In questo lavoro è presentato un nuovo metodo di studio per valutare il comportamento interparticellare durante la coalescenza e l'agglomerazione di due particelle. Il test di contatto tra le due particelle viene eseguito usando un puntale con due filamenti sui quali vengono disposte le gocce di latte. Per ogni esperimento due gocce, del peso iniziale di circa 2 mg, sono essiccate singolarmente fino al raggiungimento di un certo contenuto di acqua. Dopo che il contenuto di acqua desiderato è stato raggiunto la camera di essiccamento è stata chiusa al flusso di aria per circa 30 secondi e le particelle sono state messe in contatto portando vicino i due filamenti utilizzando un'apposita pinza, dopodiché è stato riaperto il flusso di aria per poter terminare il processo di essiccamento. Le condizioni operative dell'aria sono state: temperatura di 50, 70 e 90°C e velocità di 1m/s.

Test preliminari sono stati necessari per poter selezionare la posizione delle gocce rispetto alla direzione del flusso: la cinetica di essiccamento di una singola particella (caso I) è stata confrontata con la cinetica di essiccamento delle due particelle, posizionate in direzione ortogonale (caso II) e parallela (caso III) rispetto al flusso d'aria. Confrontando la cinetica del caso II e III con il caso I è stato possibile vedere che il caso III è più lento rispetto al caso I, invece il caso II mostra la stessa cinetica di essiccamento del caso I. Anche la morfologia delle particelle è diversa: nel caso I e nel caso II il flusso di aria incontra le due gocce allo stesso momento e mostrano la stessa morfologia, invece nel caso

III la particella che incontra prima il flusso di aria è più secca rispetto alla seconda. Per questo motivo, la cinetica di essiccamento delle gocce posizionate in parallelo è più lenta rispetto a quelle in direzione ortogonale. Queste prove preventive hanno permesso di scegliere quale delle due disposizioni avrebbe restituito la stessa morfologia e la stessa cinetica di essiccamento di una singola particella. In tal modo si è deciso di effettuare gli esperimenti ponendo le particelle ortogonalmente alla direzione del flusso d'aria (caso II).

Gli esperimenti sono stati condotti su latte fresco scremato e intero. Confrontando le cinetiche di essiccamento del latte scremato con quelle del latte intero, che hanno un simile contenuto iniziale di acqua, i risultati hanno dimostrato che il latte intero si essicca più lentamente rispetto al latte scremato. Ciò è dovuto alla presenza dei grassi, nel latte intero, che ostacola l'evaporazione dell'acqua.

I risultati dei test di contatto sia per latte scremato che per latte intero, corrispondono a tre comportamenti principali: coalescenza, adesione, e non adesione. La coalescenza si verifica quando durante il contatto una particella viene trasferita su un'altra e si possono unire formando una particella sferica più grande. L'adesione si verifica quando, dopo il contatto, le particelle cambiano la loro forma in quanto si può avere il trasferimento di materiale da una particella all'altra senza che però vi sia la formazione di un'unica particella sferica, il materiale rimane così come si è deformato, continuando l'essiccamento senza cambiare forma. La non adesione si verifica quando le particelle, dopo il contatto, si possono separare senza che vi sia una strizione e le loro forme non cambiano. Sono stati osservati quattro diversi casi di adesione, per un totale di sei casi di contatto, compresi la coalescenza e la non adesione. Le differenze tra i casi potrebbero essere correlate alle forze di adesione e/o coesione. Le forze di adesione dominano completamente durante la coalescenza, gradualmente vengono sostituite dalle forze di coesione fino a quando viene raggiunta la condizione di non adesione. A questo punto le forze coesive dominano il meccanismo, quindi la superficie delle particelle è considerata non aderente e quindi secca.

Le misure di cinetica di essiccamento delle particelle dopo il test di contatto hanno dimostrato che il dispositivo è in grado di catturare le differenze di tempo di essiccamento. Le cinetiche di essiccamento delle particelle sono state valutate solo per il latte scremato. Le particelle di latte intero dopo il test di contatto hanno mostrato una grande deformazione rispetto alla forma iniziale per questo motivo le velocità di essiccamento non sono state considerate. Confrontando i tre

comportamenti, il latte scremato a seguito della prova di contatto, in condizioni di coalescenza, ha mostrato un rallentamento della velocità di essiccamento più marcato rispetto al comportamento di adesione e non adesione. Questo è dovuto al fatto che a causa della coalescenza si è formata una goccia di dimensioni maggiori che ha un tempo di essiccazione più lungo. Gli altri due comportamenti, invece, hanno portato alla formazione di due particelle con forme e dimensioni simili alle particelle iniziali, pertanto le velocità di essiccazione sono comparabili con quelle delle particelle essiccate senza effettuare il test. La valutazione delle condizioni di coalescenza e agglomerazione è stata effettuata associando i dati sperimentali al calcolo del numero di Ohnesorge, (Oh^2), calcolato tenendo in considerazione le condizioni superficiali e alla temperatura di transizione vetrosa (T_g). Al fine di simulare le condizioni di superficie delle particelle è stato usato un modello già validato precedentemente per descrivere la cinetica di essiccamento del latte.

I test di contatto hanno dimostrato che le particelle che coalescono hanno un $Oh^2_{surface}$ inferiore a 1. Ciò risulta essere in accordo con i criteri teorici, che vengono utilizzati per la modellazione delle collisioni delle particelle durante l'essiccamento nello spray dryer. Invece, le particelle che hanno mostrato un comportamento adesivo e non adesivo avevano un $Oh^2_{surface}$ maggiore di 1. Il $\Delta T_{surface} = (T_{particle} - T_g)_{surface}$ ha mostrato che la coalescenza delle particelle si ha per $\Delta T_{surface} > 140°C$ ed esse sono adesive per $\Delta T_{surface} > 30°C$, il che è in accordo con risultati di letteratura, che mostrano che il punto di adesività dei materiali amorfi risulta essere compreso tra i 20 e i 40°C.

I risultati sperimentali combinati con il modello della cinetica di essiccamento possono essere usati per modellare il processo di essiccamento nello spray dryer. L'approccio suggerito può essere utilizzato per supportare la progettazione e lo scale-up dell'apparecchiatura, in modo tale da migliorare e controllare le proprietà del prodotto finale.

Appendix

Next is reported paper 'Coalescence and agglomeration of individual particles of skim milk during convective drying' written during thesis project at SP- Food and Bioscience (SE).

Contents lists available at ScienceDirect

Journal of Food Engineering

journal homepage: www.elsevier.com/locate/jfoodeng

ELSEVIER

Coalescence and agglomeration of individual particles of skim milk during convective drying

CrossMark

L. Malafronte [a, b], L. Ahrné [a, b, *], V. Robertiello [c], F. Innings [d], A. Rasmuson [b]

[a] Food and Bioscience, SP Technical Research Institute of Sweden, Gothenburg, Sweden
[b] Chemical and Biological Engineering, Chalmers University of Technology, Gothenburg, Sweden
[c] Department of Industrial Engineering, Università di Salerno, Salerno, Italy
[d] Tetra Pak Processing Systems, Lund, Sweden

ARTICLE INFO

ABSTRACT

This work presents a methodology, which combines experiments and modelling, for investigating the coalescence and agglomeration ability of a product and to support the modelling of product properties during spray drying. Two particles were dried simultaneously and contact tests were performed along the drying time. A validated mathematical model describing the drying kinetics of milk particles was used to predict surface conditions during contact tests. Three major mechanisms were observed, coalescence, stickiness, and non-stickiness, which were related to adhesion and cohesion forces. The simulation model allowed evaluation of the surface Ohnesorge dimensionless number and surface glass transition temperature, which showed to be good parameters for predicting contact mechanisms. The model was also used to predict shell formation in drying particles. Wet and dry shell formation was simulated over the drying time, to improve understanding of observed contact behaviour.

© 2015 Elsevier Ltd. All rights reserved.

1. Introduction

Spray drying is a unique drying technique, involving both particle formation and drying, in which powders are produced by introducing atomized liquid feed into a hot air stream. Spray drying can be considered a suspended particle processing system, as drying is performed while particles are suspended in air (Masters, 1991). It is a common process used for producing a large variety of pharmaceutical and food powders, including dairy powders. The functional properties of spray-dried powders, such as flowability and foaming, are difficult to control due to lack of knowledge of how product properties form and are changed during the spray-drying process.

Modelling is an important tool when designing and scaling up industrial spray-drying equipment, in order to reduce development time and costs. However, model validation is needed in order to achieve accurate predictions; this is a challenging task due to the dynamic (i.e., non-stationary) nature of the spray-drying process

and difficulties in sampling and monitoring particle changes during the drying process (Norton and Sun, 2006). In addition to changes in each particle, wall—particle and particle—particle collisions occur, which strongly affect the performance of the drying process and influence the morphology of the final powder and consequently functional properties. Collision between particles may lead to coalescence, agglomeration, or rebound, depending on the physical properties of individual particles at the time of collision. Coalescence occurs between liquid particles; agglomeration and rebound depend on the stickiness of the particle material, though their occurrence during spray drying is not completely understood. Some authors have modelled these mechanisms based on calculations of the physical conditions of particles (Verdurmen et al., 2004). In modelling coalescence phenomena during spray drying, the physical conditions are calculated based on theoretical assumption only, and experimental set-up for validating these assumptions has not been implemented. In modelling agglomeration phenomena, the physical conditions used are based on experimental results. Various measurement methods have been developed to characterize the agglomeration of food powders in terms of their stickiness *after* drying (Boonyai et al., 2004); however, there is a need for a methodology allowing the investigation of coalescence and agglomeration *during* spray drying.

* Corresponding author. Food and Bioscience, SP Technical Research Institute of Sweden, Gothenburg, Sweden.
E-mail address: lilia.ahrne@sp.se (L. Ahrné).

Nomenclature

c_{ext}	external vapour concentration (kg m^{-3})		u^*	maximum water mass fraction on a solid weight basis (kg kg^{-1})
c_{sat}	vapour concentration on the surface (kg m^{-3})		x	water mass fraction on a total weight basis (kg kg^{-1})
C_p	specific heat (J kg^{-1} K^{-1})		z	solid fixed coordinate (kg)
d	pure density (kg m^{-3})		ΔH_{ev}	latent heat of water evaporation (J kg^{-1})
D	diffusion coefficient (m^2 s^{-1})			
F	flux of water leaving the surface (kg m^{-2} s^{-1})		*Greek alphabet*	
h_{ext}	external heat transfer coefficient (W m^{-2} K^{-1})		ρ	density (kg m^{-3})
k	thermal conductivity (W m^{-1} K^{-1})		μ	viscosity (Pa s)
k_{ext}	external mass transfer coefficient (m s^{-1})		μ^*	minimum viscosity for wet shell formation (Pa s)
M	molecular weight of water (g mol^{-1})		σ	surface tension (N m^{-1})
Nu	Nusselt dimensionless number ($-$)			
Oh	Ohnesorge dimensionless number		*Subscripts*	
P_{sat}	vapour pressure (Pa)		0	initial value
r	radius coordinate (m)		I	Case I
R	radius of the particle (m)		II	Case II
$\underline{R}$	ideal gas constant (J K^{-1} mol^{-1})		eff	effective
Sh	Sherwood dimensionless number ($-$)		ext	external
t	time (s)		g	glass transition
T	temperature (K)		max	maximum value
TS	percentage of total solids (%)		s	solid
u	water mass fraction on a solid weight basis (kg kg^{-1})		surf	particle surface
			w	water

Adhikari et al. (2003) developed a probe tack test to determine the stickiness of individual particles on a surface during convective drying, and Haider et al. (2014) used a micromanipulation particle tester to study the deformation of two homogenous particles. These are the only two methods reported in the literature that facilitate a better understanding of the stickiness and inter-particle forces of individual particles. However, the probe tack tester focuses on the stickiness of a drying particle on a surface, while the micromanipulation particle tester concentrates on inter-particle forces but not during drying.

In our view, a pure experimental approach to studying particle coalescence and stickiness during drying is difficult due to difficulties in measuring water content and temperature profiles inside and on the surface of particles. On the other hand, a pure modelling approach cannot be used due to lack of validation of the theories applied. The goal of this work is therefore to develop a novel methodology that combines experiments and modelling to help understand the physical conditions of the coalescence and stickiness of two skim milk particles brought into contact. This knowledge will be combined to simulate the shell formation in a single particle during drying and to improve our understanding of coalescence, stickiness, and non-stickiness behaviour within the spray dryer.

2. Drying-kinetics model

The drying-kinetics model consists of heat and mass distributed parameter balances on a spherical geometry. The model was solved in solid fixed coordinates using Multiphysics® 4.3b (COMSOL, Stockholm, Sweden). The drying model and its validation are described in detail in a previous publication (Malafronte et al., 2015a).

The mass and the heat balances in solid fixed coordinates, together with the initial conditions (I.C.) and boundary conditions (B.C.), are the following:

Mass balance

$$\frac{\partial u}{\partial t} = \frac{\partial}{\partial z}\left(\rho_s^2 r^4 D_{eff}\frac{\partial u}{\partial z}\right) \tag{1}$$

$$\text{I.C. } t = 0; \; u = u_0 \tag{2}$$

$$\text{B.C. } t > 0 \; z = 0; \; \frac{\partial u}{\partial z} = 0 \tag{3}$$

$$z = z_{max} \quad -D_{eff}\rho_s\frac{\partial u}{\partial z} = \frac{F}{\rho_s R_{ext}^2} \tag{4}$$

Heat balance

$$\rho C_p\frac{\partial T}{\partial t} = k\rho_s\frac{\partial}{\partial z}\cdot\left(r^4\rho_s\frac{\partial T}{\partial z}\right) \tag{5}$$

$$\text{I.C. } t = 0; \; T = T_0 \tag{6}$$

$$\text{B.C. } t > 0 \; z = 0; \; \frac{\partial T}{\partial z} = 0 \tag{7}$$

$$z = z_{max} \quad -k\rho_s\frac{\partial T}{\partial z} = \frac{h_{ext}(T - T_{ext}) + \Delta H_{ev}(T)F}{R_{ext}^2} \tag{8}$$

where u is the mass fraction on a solid basis, r is the real coordinate, and ρ_s is the solid concentration, which equals 1248 kg$_{solid}$ m^{-3} (Singh and Heldman, 2001). D_{eff} is the effective diffusivity of water in skim milk as a function of water content and temperature:

$$D_{eff}(u,T) = 2.94 \cdot 10^{-10} exp\left(0.335 \left(1 - \frac{1}{1-(1-x_w)\frac{\rho(u)}{d_s}} \right) \right)$$
$$exp\left(-2060\left(\frac{1}{T} - \frac{1}{323} \right) \right)$$

$$(9)$$

F is the flux of water leaving the surface:

$$F = k_{ext}(c_{sat}(T) - c_{ext}) = k_{ext}\left(\frac{M \cdot P_{sat,milk}(T,c)}{\underline{R} \cdot T} - c_{ext} \right) \qquad (10)$$

$P_{sat,\,milk}$ is the saturated vapour pressure of the water in the sample; this depends on the water activity, which is calculated using experimental correlations reported by Lin et al. (2005). The conductivities and specific heats of the skim milk were calculated as functions of the water content, temperature, and composition using the expressions reported by Singh and Heldman (2001). $\Delta H_{ev}(T)$ is the latent heat of water evaporation. h_{ext} and k_{ext} are the external convective heat and mass transfer coefficients, which are evaluated during drying as a function of the dimensionless Nusselt (Nu) and Sherwood (Sh) numbers, respectively, using the empirical correlations for stationary flow around a solid sphere (Bird et al., 2007).

3. Materials and methods

3.1. Materials

Drying experiments were performed using fresh skim milk. The composition of the milk on a total weight basis is 0.9 kg_{water}/kg_{total}, 0.049 $kg_{carbohydrate}/kg_{total}$, 0.035 $kg_{protein}/kg_{total}$, and 0.0012 kg_{fat}/kg_{total}. For better analysis of particle contact tests pink food colouring was used. The minimum amount of food colouring needed to detect a difference in colour between particles was used and preliminary particle contact tests have been performed without food colouring showing that food colouring do not influence results; 10 mL of fresh milk was stained with 0.025 mL of colouring. The fresh skim milk and food colouring were commercial products purchased in local stores.

3.2. Particle contact test

The drying-kinetics device developed by Malafronte et al. (2015a) for drying single particles was adapted for drying two individual particles at the same time. A suspended system consisting of two metallic filaments was developed to allow the simultaneous drying of two particles as shown in Fig. 1. For each experiment, two particles with an initial total weight of approximately 4 mg (each particle weighed approximately 2 mg) were created using a

micropipette and held at the tips of the metallic filaments. The metallic filaments were held below a microbalance (Mettler Toledo's XP6 Micro Balance, maximum capacity 6.1 g, readability 0.1 μg and minimum weight typical 0.82 mg) and weight was recorded with a minimum step of 0.1 s using a dedicated software (LabX 2012 Client). Drying was performed at three different air temperatures (i.e., 50, 70, and 90 °C), an air humidity of 0.007 $kg_{water}/kg_{dry\ air}$, and an air velocity of 1 m s^{-1}.

Particles were dried individually until a certain water content was reached, after which they were brought into contact by bringing close the tips of the filaments using tweezers. Drying was then continued. Particles were brought into contact at five different average water contents, x_w, i.e., 85, 80, 75, 70, and 65% (on a total basis). The drying time needed to reach the desired average water content was calculated using the drying-kinetics model reported by Malafronte et al. (2015a). Experiments were performed in triplicate. The experimental steps are the following:

1. the air system is turned on until the desired air temperature is reached;
2. the balance is stabilized for a minimum of 15 min (in each weighing experiment);
3. the airflow is deflected from the measurement chamber;
4. two individual particles are placed on at the tips of the metallic filaments;
5. the weight of the particles is recorded for 10 s without airflow;
6. the airflow is again directed to the measurement chamber and the weight recording starts;
7. when the desired water content is reached, the airflow is deflected from the measurement chamber;
8. the drying chamber is opened and the particles are brought into contact; and
9. the drying chamber is closed and the airflow is again directed to the measurement chamber.

The particle weight was recorded from steps 5 to 9, corresponding to a total drying time of 1000 s. The duration of step 8 was 30 s.

3.3. Analysis of particle contact test

Experimental results of particle contact tests were analysed as a function of the glass transition temperature, T_g, dynamic viscosity, μ, and Ohnesorge dimensionless number, Oh. T_g, μ, and Oh^2 were calculated as a function of the surface and average water content and temperature of the particles during drying, which were simulated using the drying-kinetics model.

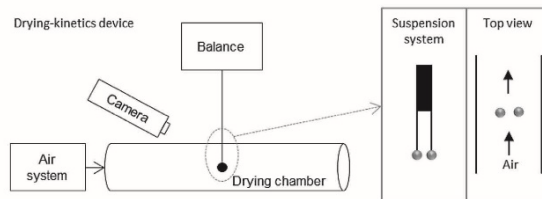The glass transition temperature of skim milk, T_g, is (Vuataz, 2002):

Fig. 1. Sketch of the drying-kinetics device.

$$T_g = \frac{\left(TS_{particle}\right) \cdot 101 + 6.5 \cdot \left(100 - TS_{particle}\right) \cdot (-135)}{TS + 6.5 \cdot \left(100 - TS_{particle}\right)} \quad (11)$$

where $TS_{particle}$ is the percentage of solids in the particle. The dynamic viscosity as a function of the water content and temperature of the particle is calculated using the following correlation valid for amorphous food materials (Roos, 1995):

$$\frac{\log(\mu)}{\log(\mu_g)} = \frac{-17.44 \cdot (T - T_g)}{51.6 + (T - T_g)} \quad (12)$$

where μ_g is the viscosity at the glass transition temperature, which is considered to equal 10^{12} Pa s.

The Ohnesorge dimensionless number (Oh) represents the ratio between viscous and surface tension forces (Verdurmen et al., 2004). If $Oh^2 < 1$, particles coalesce; if $Oh^2 > 1$, particles might agglomerate. Oh^2 is calculated as follows:

$$Oh^2 = \frac{\mu^2}{2 \cdot R_{ext} \cdot \rho \cdot \sigma} \quad (13)$$

where μ and σ are the dynamic viscosity and surface tension, respectively, of skim milk. The surface tension of skim milk is considered constant and equal to 46×10^{-3} N m^{-1} (Whitnah, 1959).

3.4. Shell formation

Shell formation in a single drying particle has been simulated to help understand the coalescence, stickiness, and non-stickiness mechanisms. Skim milk is a skin-forming material, since solid precipitation occurs rapidly at the beginning of the drying process covering the whole surface of the particle. During drying time, the skin thickens, dries-out and hardens, promoting the formation of a solid particle (Nešić and Vodnik, 1991; Walton, 2000). Based on the water content, the skin has been considered as a wet (moist) or dry shell; a wet shell is a shell that is deformable and easily penetrated by water, while a dry shell hinders water diffusion and the shrinkage or collapse of particles (Handscomb et al., 2009b). Criteria for wet and dry shell formation have been investigated, as described below.

The drying kinetics model of Malafronte et al. (2015a) and summarized above has been used to simulate the average and internal water contents and temperature profiles and to calculate the dynamic viscosity, μ, as a function of the particle radius. The wet shell is defined as the volume of a particle with a viscosity higher than a minimum value, μ^*. This minimum value is defined as the surface viscosity of a particle at which $Oh^2_{surf} > 1$. The dry shell is defined as the volume of a particle with a water content below a maximum water content, u^*. Two cases of dry shell formation have been investigated, corresponding to two maximum water content values: u_I^* (Case I) and u_{II}^* (Case II). Case I, u_I^*, is the surface water content at which the particle temperature exceeds the wet bulb temperature. A rapid increase of temperature is in fact observed due to the formation of a dry shell, which increases the resistance to mass transfer and thus reduces the evaporation rate (Handscomb et al., 2009a; Nešić and Vodnik, 1991). In contrast, Case II, u_{II}^*, is the surface water content at which particles are non-sticky. The thickening of wet and dry shells occurs gradually. When the wet shell reaches the centre of the particle, a soft core is formed. When the dry shell reaches the centre of the particle, a solid particle is formed.

4. Results

4.1. Behaviour of particles during the contact test

Particle contact tests were performed at five average water contents (i.e., 85, 80, 75, 70, and 65% on a total weight basis) and at three drying temperatures (i.e., 50, 70, and 90 °C). The drying time needed to reach the desired average water content was calculated using the drying-kinetics model. The range of water contents has been chosen based on preliminary experiments in order to investigate the transition from coalescence to non-stickiness behaviours. The drying temperatures have been chosen based on the range of validation of the drying-kinetics model. Table 1 shows the drying times. Fig. 2 shows typical images of two particles before, during, and after contact tests. The particle behaviour during the contact tests was divided into three major mechanisms: coalescence, stickiness, and non-stickiness. Coalescence occurs when, after contact, a particle merges with another particle. Stickiness occurs when, after contact, "necking" appears at the particle–particle interface when the particles are separating. Separation can cause particle deformation or breakage. Non-stickiness is found when, after contact, particles separate without necking and retain their original shape. Neck formation – expected when moist particles are brought into contact – occurs through the formation of a liquid bridge due to the low viscosity of the surface liquid at the particle–particle interface. As the particle dries, viscosity increases and limits the mobility of the liquid, which cannot form bridges at the particle–particle interface, so a neck is not formed (Schulze, 2007). The mechanisms of coalescence, stickiness, and non-stickiness can be related to the adhesion and cohesion forces (Adhikari et al., 2003). Adhesion is defined as the attraction force between two particles that acts to hold their surfaces together. Cohesion is an attraction force within a particle that acts to unite its parts. Hence, coalescence can be considered a mechanism completely dominated by adhesion forces (Case 1). Stickiness is instead characterized by both adhesion and cohesion forces. Four cases can be observed in the stickiness regime: adhesion-cohesion with adhesion dominance, adhesion-cohesion with equal dominance, adhesion-cohesion with cohesion dominance, and cohesion with a sticky surface (from Cases 2 to 5). Distinguishing between the dominance of adhesion versus cohesion can be done by observing the size of the neck that forms at the particle–particle interface when the particles are separating, i.e., the smaller the neck, the more cohesive the particles. Non-stickiness behaviour is completely dominated by cohesive forces (Case 6); it is distinguished from Case 5 because necking does not occur, so the particle surface is considered non-sticky. Fig. 3 presents an overview of the average water content as a function of the particle contact behaviour at the three operating temperatures. As expected, the results indicate that particles tend to be non-sticky at lower average water contents, while at high water contents, particles tend to coalesce.

4.2. Drying kinetics of particles before and after the contact test

Drying kinetics were measured for all particles before and after contact tests and for particles not undergoing contact tests. Measurements were performed at air temperatures of 50, 70, and 90 °C and an air velocity of 1 m s^{-1}. Fig. 4 shows an example of the drying rates at 90 °C. Drying rates were calculated by fitting each experimental drying kinetics curve with a fourth-order polynomial with a coefficient of determination greater than 0.99 as suggested by Malafronte et al. (2015b). Results indicate that particles exhibiting coalescence behaviour have a lower drying rate after the contact test, as contact leads to the formation of bigger particles (Fig. 2 – Case 1). Particles that exhibit sticky or non-sticky behaviour display

Table 1
Simulated drying times at which particle contact tests were performed.

T, [°C]	50					70					90				
x_w, [%]	85	80	75	70	65	85	80	75	70	65	85	80	75	70	65
t, [s]	68	108	136	156	173	42	66	83	96	110	29	46	58	69	79
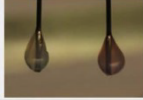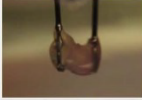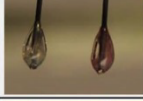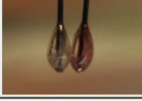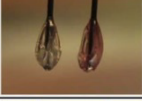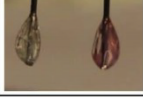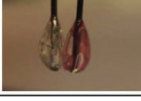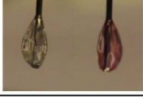
Mechanism	Case	Contact			Forces
		Before	Necking	After	
Coalescence	1				Adhesion
Stickiness	2				Adhesion-Cohesion with adhesion dominance
	3				Adhesion-Cohesion with equal dominance
	4				Adhesion-Cohesion with cohesion dominance
	5				Cohesion with sticky surface
Non-stickiness	6				Cohesion with non-sticky surface

Fig. 2. Classification of mechanisms observed during particle contact tests.

drying rates similar to those of particles not undergoing contact tests; stickiness and non-stickiness lead to the formation of two individual particles whose size and shape are similar to those of particles before contact tests and with negligible mass exchange between them.

4.3. Simulation of coalescence and stickiness conditions

The drying-kinetics simulation model was used to predict the surface and average water contents and temperature of the particles at the contact test experimental points. The simulation results allow estimation of the Ohnesorge dimensionless number, Oh^2, dynamic viscosity, μ, and glass transition temperature, T_g. Oh^2 is calculated as a function of the surface, Oh^2_{surf}, and average, $Oh^2_{average}$,

water contents and temperature of particles. The calculated $Oh^2_{average}$ is always below 1 at 50, 70, and 90 °C and in all particle contact cases. Oh^2_{surf} is shown in Fig. 5; for each particle contact case, Oh^2_{surf} is shown at the three operating temperatures. The results indicate that coalescence occurs when Oh^2_{surf} is below 1; in the case of stickiness and non-stickiness, Oh^2_{surf} always exceeds 1. Oh^2_{surf} results are in agreement with a particle classification used in modelling particle collision during spray drying (Verdurmen et al., 2004). If $Oh^2 < 1$, particles are assumed to be dominated by surface tension forces and particle contact results in the formation of a new spherical particle; if $Oh^2 > 1$, particles are dominated by viscous forces and can exhibit stickiness or non-stickiness behaviour. Hence, evaluation of Oh^2_{surf} is needed in order to predict coalescence mechanisms.

Fig. 3. Particle contact test results in terms of average water content of the particle as a function of the particle contact case.

Fig. 4. Drying rates as a function of the water content on a solid weight basis at an air temperature of 90 °C for particles after contact testing and for two individual particles not contact tested.
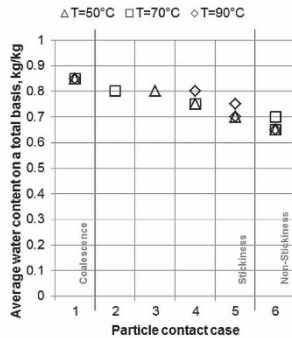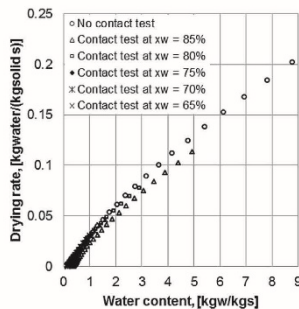
Sticky and non-sticky amorphous particles are usually distinguished based on the value of $\Delta T = T - T_g$ (Palzer, 2009). Also in the present case, ΔT is estimated as a function of the water content and temperature calculated at the surface, ΔT_{surf}, and as the whole particle average, $\Delta T_{average}$. $\Delta T_{average}$ results always exceed 140 °C at the three operating temperatures and in all particle contact cases. ΔT_{surf} is shown in Fig. 6; ΔT_{surf} values are shown for each particle contact case at the three operating temperatures. Results indicate that coalescence occurs when $\Delta T_{surf} \approx 140$ °C; non-stickiness occurs when $\Delta T_{surf} < 30$ °C. The ΔT_{surf} of particles exhibiting stickiness varies the most, from a minimum of 20 °C to a maximum of 130 °C. Sticky particles, which have a ΔT_{surf} of approximately 20 °C, exhibit a stickiness mechanism (Case 5). As skim milk is a shell-forming material, the particle surface dries much faster than does the inner part; during contact between particles, inner material might wet the surface, causing stickiness. For this reason, a net distinction in terms of ΔT_{surf} between stickiness and non-stickiness cannot be observed. However, ΔT_{surf} results for non-sticky particles indicate that particles are sticky when ΔT_{surf} exceeds 30 °C. ΔT_{surf} results are in agreement with literature findings, the sticky point of
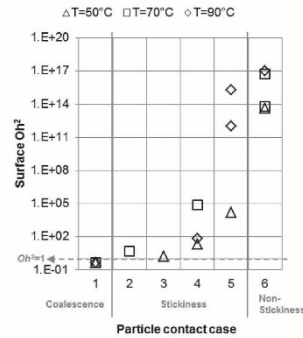

Fig. 5. Surface Ohnesorge dimensionless number as a function of the particle contact case and drying temperature.

amorphous materials varying between 20 and 40 °C; stickiness experiments with skim milk powders obtained using a particle gun method find a sticky point at approximately 40 °C (Paterson et al., 2007). Hence, also in this case, evaluation of ΔT_{surf} is needed in order to predict agglomeration mechanisms, and the sticky point is obtained for $\Delta T_{surf} > 30$ °C.

4.4. Determination of shell formation during drying

The drying-kinetics modelling simulation (Malafronte et al., 2015a) clearly demonstrates the existence of a water profile in the particle during drying. Furthermore, when analysing particle behaviour during the contact tests, it was observed that the inside of the particles is more liquid than the surface. Because skim milk is a shell-forming material (Nešić and Vodnik, 1991; Walton, 2000), the formation of a hard/dried surface (i.e., shell) is expected; this shell increases in thickness during the drying process until it reaches the centre and the particle is fully dried. This work assumes the existence of a wet shell between the liquid core and the dry shell.

A wet shell appears when the viscosity is higher than the surface viscosity of particles at which $Oh_{surf}^2 > 1$. Two cases of dry shell formation were considered: u_I^* (Case I) and u_{II}^* (Case II). The maximum surface water content, u_I^*, at which the particle temperature exceeds the wet bulb temperature is approximately 0.18–0.21 kg_{water}/kg_{solids} at 50, 70, and 90 °C. Hence, 0.2 kg_{water}/kg_{solids} is assumed to be the maximum water content at which particles can be considered dry. Instead, the maximum surface water content, u_{II}^*, at which particles are non-sticky is 0.11 kg_{water}/kg_{solids}.

Fig. 7 shows the wet and dry shell formation at a temperature of 70 °C. The plot shows the particle radius as a function of time and the development of the wet and dry shells over the drying time. In this case, the dry shell criteria, u_I^*, is applied. Shrinkage occurs during drying, so the external particle radius decreases with time. From 0 to 50 s, the particle can be considered fully liquid; at 50 s, a wet shell appears followed by the formation of a dry shell at 90 s. After shell formation, wet and dry shell thickening is observed. During wet shell thickening, the particle displays a liquid core covered by a wet shell until the wet shell reaches the centre of the particle ($t \approx 310$ s); at this point, a soft core forms, which is covered by a dry shell. When the dry shell reaches the centre, the particle can be considered fully dry ($t \approx 450$ s). Microscopy of morphology
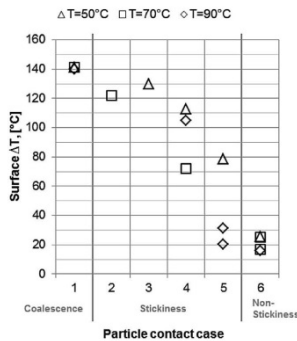
Fig. 6. Surface $\Delta T = T - T_g$ as a function of the particle contact case and drying temperature.

changes over time for a single drop indicates that the particle shrinks spherically up to 80 s and then folds between 80 and 160 s; after 160 s, the particle morphology does not change. Morphology changes seem to validate the hypothesis of wet and dry shell formation; folding occurs when a wet shell covers the particle, and the thicker the dry shell folding reduces. Comparing the results of particle contact tests with the shell formation process, it is possible to observe stickiness when a wet shell covers the liquid particle; a

thin dry shell instead appears at the end of the sticky period. The thicker the dry shell, the more non-sticky behaviour the particle displays.

In Fig. 8 shell formation is compared with the drying rate as a function of the average water content at the three temperatures investigated. In this figure, the wet and dry shell radii are normalized with the external radius of the particle. It is possible to see that particles have two falling-drying-rate periods (i.e., Periods 1 and 2) at 50, 70, and 90 °C, the lower the drying temperature, the lower the drying rate. In all cases, wet shell formation begins during the first falling-drying-rate period (Period 1), a dry shell appearing when the second falling period (Period 2) starts. Simulations also indicate that the lower the drying rate, the thicker the wet shell, as drying is slower and the wet shell has time to develop. At each temperature, the wet shell thickens faster during the first than the second falling period.

The same study was performed using u_{II}^* as the maximum water content for dry shell formation (Case II). Fig. 9 compares dry shell formation in Cases I and II. The results indicate that in both cases dry shell formation starts at approximately the same time and, as expected, that a thicker dry shell forms at a high u^* (Case II). Prediction of shell formation within the particle is strongly dependent on the criteria chosen for the formation of the wet and dry shells and further validation is needed.

In addition, microscopy of a single particle during drying at 70 °C indicates that the particle shrinks spherically until 120 s, folding occurring after this time (Fig. 7). The simulation model used here describes the drying kinetics of a single spherical particle. Therefore, the model more accurately predicts surface conditions in the spherical shrinkage period, during which particle contact tests are performed.
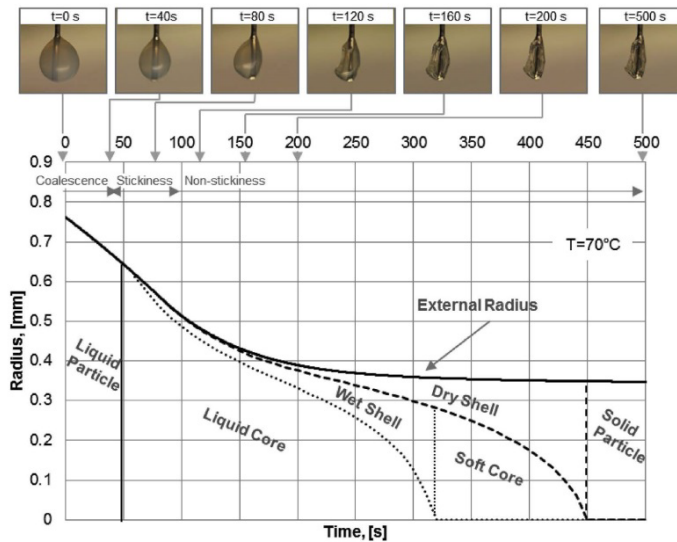

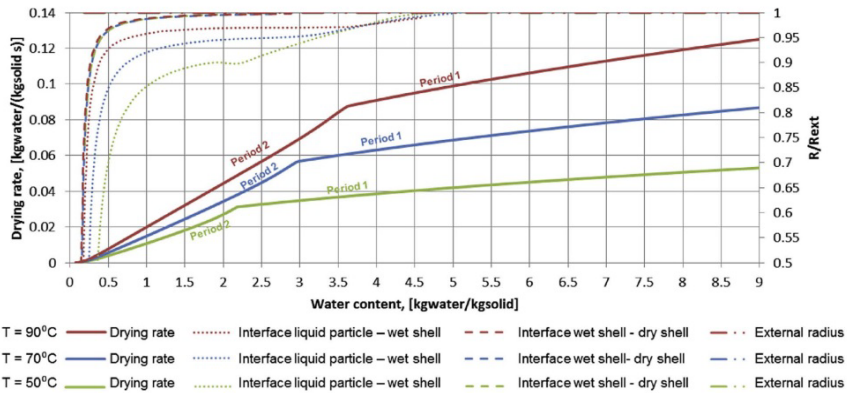**Fig. 7.** Simulation of shell formation in a particle drying at 70 °C.

Fig. 8. Comparison between drying rate and thickening of wet and dry shells at 50, 70, and 90 °C. The wet shell is the distance between the liquid particle—wet shell interface and the wet shell—dry shell interface. The dry shell is the distance between the wet shell—dry shell interface and the external radius. The interfaces and external radius are expressed in terms of the normalized radius (right axis). The drying rate is shown on the left axis.
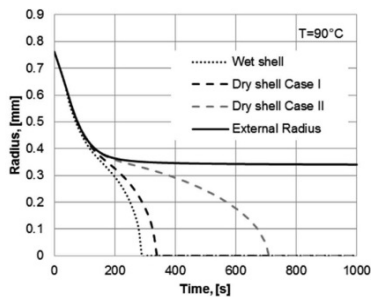

Fig. 9. Simulated shell formation in a particle drying at 90 °C in two dry shell cases: $u_I = 0.2$ kg$_{water}$/kg$_{solid}$ (Case I) and $u_{II} = 0.11$ kg$_{water}$/kg$_{solid}$ (Case II).

5. Conclusions

This paper reports the development of a novel methodology combining experimental and modelling approaches suitable for advancing understanding of inter-particle coalescence, stickiness, and non-stickiness behaviour during drying. Specifically, the tools developed in this paper can be implemented in modelling the spray-drying process used for designing and scaling-up the process and for enhancing and controlling the functional properties of powders.

In this work a drying-kinetics device was successfully used to dry two particles of skim milk simultaneously, and to perform particle contact tests and a validated drying-kinetics model was used to simulate the surface conditions of particles during contact tests. Particle contact tests demonstrated that it was possible to distinguish between three major mechanisms, i.e., coalescence, stickiness, and non-stickiness that could be related to adhesion and

cohesion forces. Adhesion forces completely dominated during coalescence and gradually declining until non-stickiness was observed, at which point cohesive forces dominated the mechanism. Simulated surface conditions of particles at contact test experimental points indicated the effect of surface conditions (i.e., water content and temperature) on the coalescence and stickiness behaviour of the particles and underline the importance of estimating the surface properties of particles when investigating coalescence and stickiness conditions. Coalescence occurs when Oh_{surf}^2 is below 1. In contrast, stickiness and non-stickiness occur when Oh_{surf}^2 exceeds 1. These results validated the theoretical criteria used when modelling particle collision during spray drying. Calculation of $\Delta T_{surf} = (T - T_g)_{surf}$ indicated that skim milk particles coalesced at $\Delta T_{surf} > 140$ °C and were sticky at $\Delta T_{surf} > 30$ °C. Simulation of shell formation in a drying particle indicates the existence of wet and dry shells and that the wet shell thickening occurring during stickiness is followed by dry shell thickening during non-stickiness.

Measurements of drying kinetics of particles after contact tests indicated that the drying-kinetics device could capture differences in drying time. Particles displaying a coalescence mechanism had a lower drying rate after contact testing than sticky or non-sticky particles. Coalescence led to the formation of bigger particles and, consequently, to a longer drying time.

References

Adhikari, B., Howes, T., Bhandari, B.R., Truong, V., 2003. In situ characterization of stickiness of sugar-rich foods using a linear actuator driven stickiness testing device. J. Food Eng. 58 (1), 11–22.
Bird, R.B., Stewart, W.E., Lightfoot, E.N., 2007. Transport Phenomena. Wiley.
Boonyai, P., Bhandari, B., Howes, T., 2004. Stickiness measurement techniques for food powders: a review. Powder Technol. 145 (1), 34–46.
Haider, C.I., Hounslow, M.J., Salman, A.D., Althaus, T.O., Niederreiter, G., Palzer, S.,

2014. Influence of environmental conditions on caking mechanisms in individual amorphous food particle contacts. AIChE J. 60 (8), 2774–2787.

Handscomb, C.S., Kraft, M., Bayly, A.E., 2009a. A new model for the drying of droplets containing suspended solids. Chem. Eng. Sci. 64 (4), 628–637.

Handscomb, C.S., Kraft, M., Bayly, A.E., 2009b. A new model for the drying of droplets containing suspended solids after shell formation. Chem. Eng. Sci. 64 (2), 228–246.

Lin, S.X.Q., Chen, X.D., Pearce, D.L., 2005. Desorption isotherm of milk powders at elevated temperatures and over a wide range of relative humidity. J. Food Eng. 68 (2), 257–264.

Malafronte, L., Ahrné, L., Kaunisto, E., Innings, F., Rasmuson, A., 2015a. Estimation of the effective diffusion coefficient of water in skim milk during single-drop drying. J. Food Eng. 147 (0), 111–119.

Malafronte, L., Ahrné, L., Schuster, E., Innings, F., Rasmuson, A., 2015b. Exploring drying kinetics and morphology of commercial dairy powders. J. Food Eng. 158 (0), 58–65.

Masters, K., 1991. Spray Drying Handbook. Longman Scientific & Technical.

Nešić, S., Vodnik, J., 1991. Kinetics of droplet evaporation. Chem. Eng. Sci. 46 (2), 527–537.

Norton, T., Sun, D.-W., 2006. Computational fluid dynamics (CFD) – an effective and efficient design and analysis tool for the food industry: a review. Trends Food Sci. Technol. 17 (11), 600–620.

Palzer, S., 2009. Influence of material properties on the agglomeration of water-soluble amorphous particles. Powder Technol. 189 (2), 318–326.

Paterson, A.H., Bronlund, J.E., Zuo, J.Y., Chatterjee, R., 2007. Analysis of particle-gun-derived dairy powder stickiness curves. Int. Dairy J. 17 (7), 860–865.

Roos, Y., 1995. Characterization of food polymers using state diagrams. J. Food Eng. 24 (3), 339–360.

Schulze, D., 2007. Powders and Bulk Solids. Springer.

Singh, R.P., Heldman, D.R., 2001. Introduction to Food Engineering. Elsevier Science.

Verdurmen, R.E.M., Menn, P., Ritzert, J., Blei, S., Nhumaio, G.C.S., Sonne Sørensen, T., Gunsing, M., Straatsma, J., Verschueren, M., Sibeijn, M., Schulte, G., Fritsching, U., Bauckhage, K., Tropea, C., Sommerfeld, M., Watkins, A.P., Yule, A.J., Schønfeldt, H., 2004. Simulation of agglomeration in spray drying installations: the EDECAD project. Dry. Technol. 22 (6), 1403–1461.

Vuataz, G., 2002. The phase diagram of milk: a new tool for optimising the drying process. Le. Lait. 82 (4), 485–500.

Walton, D.E., 2000. The morphology of spray-dried particles a qualitative view. Dry. Technol. 18 (9), 1943–1986.

Whitnah, C.H., 1959. The surface tension of milk. A review1.2. J. Dairy Sci. 42 (9), 1437–1449.

Bibliography

1. Keshani, S., Daud, W. R. W., Nourouzi, M. M., Namvar, F. & Ghasemi, M. Spray drying: An overview on wall deposition, process and modeling. *J. Food Eng.* **146,** 152–162 (2015).

2. Turchiuli, C., Gianfrancesco, a., Palzer, S. & Dumoulin, E. Evolution of particle properties during spray drying in relation with stickiness and agglomeration control. *Powder Technol.* **208,** 433–440 (2011).

3. GEA Niro. Spray Drying Agglomeration. 1–5 at <http://www.niro.com>

4. Adhikari, B., Howes, T., Bhandari, B. R. & Truong, V. STICKINESS IN FOODS: A REVIEW OF MECHANISMS AND TEST METHODS. *Int. J. Food Prop.* **4,** 1–33 (2001).

5. Dopfer, D. *et al.* Adhesion mechanisms between water soluble particles. *Powder Technol.* **238,** 35–49 (2013).

6. Boonyai, P., Bhandari, B. & Howes, T. Stickiness measurement techniques for food powders: A review. *Powder Technol.* **145,** 34–46 (2004).

7. Palzer, S. Influence of material properties on the agglomeration of water-soluble amorphous particles. *Powder Technol.* **189,** 318–326 (2009).

8. Murti, R. a., Paterson, a. (Tony) H. J., Pearce, D. L. & Bronlund, J. E. Stickiness of skim milk powder using the particle gun technique. *Int. Dairy J.* **19,** 137–141 (2009).

9. Adhikari, B., Howes, T., Bhandari, B. R. & Truong, V. In situ characterization of stickiness of sugar-rich foods using a linear actuator driven stickiness testing device. *J. Food Eng.* **58,** 11–22 (2003).

10. Zuo, J. Y., Paterson, A. H., Bronlund, J. E. & Chatterjee, R. Using a particle-gun to measure initiation of stickiness of dairy powders. *Int. Dairy J.* **17,** 268–273 (2007).

11. Murti, R. a., Paterson, a. (Tony) H. J., Pearce, D. & Bronlund, J. E. The influence of particle velocity on the stickiness of milk powder. *Int. Dairy J.* **20,** 121–127 (2010).

12. Adhikari, B., Howes, T., Shrestha, a. K. & Bhandari, B. R. Development of stickiness of whey protein isolate and lactose droplets during convective drying. *Chem. Eng. Process. Process Intensif.* **46,** 420–428 (2007).

13. Malafronte, L., Ahrné, L., Kaunisto, E., Innings, F. & Rasmuson, A. Estimation of the effective diffusion coefficient of water in skim milk during single-drop drying. *J. Food Eng.* **147,** 111–119 (2015).

14. Singh, R. P. & Heldman, D. R. *Introduction to Food Engineering*. (Academic Press, 2001). at <https://books.google.se/books?id=xXZh9qugyGgC>

15. Perry, R. H., Green, D. W. & Maloney, J. O. *Perry's Chemical Engineers' Handbook Seventh. Society* **27,** 2735 (1997).

16. Lin, S. X. Q., Chen, X. D. & Pearce, D. L. Desorption isotherm of milk powders at elevated temperatures and over a wide range of relative humidity. *J. Food Eng.* **68,** 257–264 (2005).

17. Bird, R., Stewart, W. & Lightfoot, E. *Transport phenomena*. 914 (2006). at <http://books.google.com/books?hl=en&lr=&id=L5FnNlIaGfcC&oi=fnd&pg=PR13&dq=Transport+Phenomena&ots=LHh6k6nTlE&sig=wLfqYRKf9ITlizIAdziJEX_7NH0>

18. Vuataz, G. The phase diagram of milk: A new tool for optimising the drying process. *Lait* **82,** 485–500 (2002).

19. Roos, Y. Characterization of food polymers using state diagrams. *J. Food Eng.* **24,** 339–360 (1995).

20. Verdurmen, R. E. M. *et al.* Simulation of agglomeration in spray drying installations: The EDECAD project. *Dry. Technol.* **22,** 1403–1461 (2004).

21. Malafronte, L., Ahrné, L., Schuster, E., Innings, F. & Rasmuson, A. Exploring drying kinetics and morphology of commercial dairy powders. *J. Food Eng.* **158,** 58–65 (2015).

22. Schulze, D. *Powders and Bulk Solids: Behavior, Characterization, Storage and Flow*. (Springer Berlin Heidelberg, 2007). at <https://books.google.se/books?id=pGxWO47yA1MC>

23.   Walton, D. E. the Morphology of Spray-Dried Particles a Qualitative View. *Dry. Technol.* **18,** 1943–1986 (2000).

Acknowledgements

…Consuetudine diffusa di quando si raggiunge un traguardo è voltarsi indietro e ripercorrere tutti i momenti che ti hanno portata fino a li. Soffermandomi a ripensare ai momenti fino ad ora trascorsi, mi rendo conto che è stato fatto parecchio, ma c'è molto altro da fare, ma certo fin qui non sarei riuscita ad arrivarci da solo. Senza le spalle forti di mia madre e di mio padre credo che non sarei mai arrivata qui oggi, sono stati sempre al mio fianco pronti a sostenermi in qualsiasi momento, ponendo in me la loro totale fiducia e a sacrificarsi sotto ogni punto di vista, ed altresì presenti anche nei momenti felici e di celebrazione. Credo che non smetterò mai di ringraziarli perché senza loro oggi non sarei qui a vivere questo momento di gioia.

Le persone che ho incontrato in questi anni, hanno lasciato tutte un segno in me, permettendomi di crescere sotto ogni punto di vista. Tra quelle un grazie va soprattutto al prof. Gaetano Lamberti affiancato dalla prof. Anna Angela Barba che mi hanno accolta nella loro grande 'famiglia', ponendo così, stima e fiducia in me, permettendomi di lavorare con loro, e di portare con me un sereno ricordo di questi anni.

Una delle esperienze più significative di questi anni di studio è stato il mio soggiorno all'estero, durante il quale ho avuto modo di conoscere 'Colei che è la dimostrazione di dove può arrivare un ingegnere alimentare' (cit.), Loredana Malafronte, che oltre a guidarmi nel progetto di tesi, è diventata un esempio, un'amica, una di quelle persone che, pur senza volerlo, mi ha dato tanto.

Un grazie speciale va alla professoressa Lilia Ahrné, per avermi dato la possibilità di lavorare nel suo gruppo di ricerca facendomi vivere un'esperienza unica, facendomi sentire a casa ogni giorno trascorso all'SP.

Devo ammettere che durante questi anni è cambiato molto anche il mio carattere, sono diventata più forte, più sicura di me, ma soprattutto più testarda. E di questo qualcuno ne sa qualcosa, ebbene sì. Colui che mi ha scelta e mi continua a scegliere ogni giorno nonostante il mio carattere, a cui devo un immenso Grazie per aver avuto la pazienza di sopportarmi fino ad oggi. Grazie Carmine per aver condiviso con me tutto questo!

Gerarda, Milena, Ilaria, con ognuna di voi ho condiviso momenti ed esperienze diverse, ma tutte vi ho incontrate sul cammino dello studio, grazie per esserci state sempre in questi anni, che mi avete confortato nei momenti meno belli e supportato nei momenti di gioia. Grazie!

In questi anni ho cercato di prendere esempio da qualsiasi esperienza in cu mi sono imbattuta, cercando di prendere sempre il meglio da chiunque abbia incontrato, facendomi ritrovare la persona che sono oggi, cosciente di ciò che è e ben convinta

di ciò che vuol diventare. A voi tutti che credete in me, un grazie sincero, di cuore, per aver condiviso parte del vostro tempo insieme a me, ed aver reso il mio percorso fino ad ora, il più interessante e piacevole possibile.